6th Micro and Nano Flows Conference
Atlanta, USA, 9-12 September 2018

Flow Regime Mapping of Small-Scale Gas-Solid Fluidized Beds

Jonathan R McDONOUGH [1,*], Richard LAW [1], David A REAY [1], Vladimir ZIVKOVIC [1]

* Corresponding author: Tel.: ++44 (0)191 208 5747; Email: jonathan.mcdonough@ncl.ac.uk
1. School of Engineering, Merz Court, Newcastle University, Newcastle upon Tyne, UK

Keywords: Mini-fluidized bed, bubbling, slugging, additive manufacturing, carbon capture

The present research is part of a collaborative EPSRC project [EP/N024540/1] involving the development of tailored hydrotalcite materials for CO_2 capture from industrial processes, and the development of a novel fluidized bed process that can address the heat and mass transfer challenges of capturing CO_2 via solid adsorption. One of the experimental objectives for this project is to screen the adsorption and desorption kinetics of the hydrotalcite materials in a fluidized bed environment, requiring the identification of a suitable fluidized bed configuration and corresponding operating conditions. Thus, in this work, we present the results of flow regime mapping experiments performed in various sized 3D printed fluidized beds (hydraulic diameters of 3–15 mm) containing four different particles exhibiting Geldart A and B behavior. Using high speed camera videos and pressure drop data, we identify preliminary flow regime boundaries on a plot of dimensionless length scale (D_h/D_p) vs gas velocity (U_g).

1. Background/Motivation

Industrial processes (such as cement production, iron/steel production and petrochemical refining) account for 25% of the total CO_2 emissions produced in the EU. Although there is still scope to reduce CO_2 emissions from these processes by improving the energy efficiency through process integration, this is likely to be insufficient to meet the EU target of reducing CO_2 emissions by 80–95% by 2050 [1]. Thus, for the short term, carbon capture is likely to play a major role, at least until renewable technologies take over from fossil fuels.

Liquid based absorption has received the most attention to date for carbon capture, especially from power plant CO_2 emissions [2]. Instead, in this EPSRC collaborative project between Heriot-Watt University, Sheffield University and Newcastle University, solid based adsorption using novel hydrotalcite sorbents is being considered. An advantage of solid sorbents compared to liquids is the ability to tailor their behavior [3], making them widely applicable for the different CO_2 sources produced in each industry. At Newcastle University, the main goal is to develop an intensified solution for carbon capture using a TSA-based process involving fluidized beds and/or swirling fluidized beds.

However, it has been shown that the flow regime in fluidized beds can influence the reaction kinetics, including adsorption [4]. Although different flow regimes have been identified in the literature [5], there is limited understanding about the operating conditions responsible for producing each regime. Thus, prior to the screening of different hydrotalcite materials, the aim of the present study was to identify flow regime boundaries in various fluidized bed configurations using pressure drop data and high-speed imaging.

2. Methodology

Six planar fluidized bed geometries were considered for the development of the flow regime maps. The designs had hydraulic diameters (D_h) ranging from 3–15 mm, giving corresponding gas flow areas of 9–225 mm^2. An example fluidized bed is shown in Figure 1. Each design included a planar distributor consisting of 1 mm width square holes, above which, a 26 µm aperture steel mesh was fitted to hold the particles. A basic plenum packed with glass wool was positioned below the distributor plate. Each design was fabricated via additive manufacturing using the stereolithographic (SLA) approach using a Form2 printer (clear resin). This allowed rapid and cheap construction with high customization. To enable visualization of the flow regimes using a high-speed camera, the fluidized beds were printed three-sided, with the fourth side sealed using a sheet of Perspex.

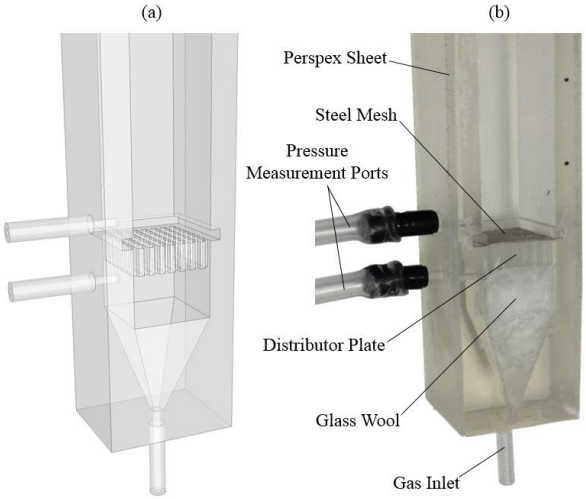

Figure 1. *Example fluidized bed design (15x15 mm cross-section) (a) CAD rendering, and (b) final 3D printed product*

Three differently sized glass microspheres (2.1 g/cm^3) and one size of silica particle (2.65 g/cm^3) were used in the present investigation. Each of the size distributions was confirmed using a Coulter LS230 sizer. The silica particles had an average size of 93 ± 10 µm (Geldart A), whilst the three glass microsphere samples had average sizes of 82 ± 7 µm (Geldart A), 170 ± 24 µm (Geldart B) and 183 ± 29 µm (Geldart B). Each of the particle sizes was normally distributed. Three particle bed heights were considered in each of the six fluidized bed designs, corresponding to static height ratios of H_s/D_h = 2, 3 and 4.

High-speed videos of the fluidized beds were recorded using a Basler acA1300-200uc camera (169 fps, 1.3 MP) fitted with a COSMICAR Television lens (12.5 mm, 1:14), monitored via Pylon Viewer software. Illumination of the beds was achieved using an LED light panel placed behind the bed and a fiber optic directional lamp (Microlight 150) pointed at the fluidized particles. A Sensirion SDP610 differential pressure transducer was used to measure the pressure drops. Here, the sensor was connected to two of the pressure ports integrated into the 3D printed design (see Figure 1). The pressure sensor had a working range of ±500 Pa, a precision of 0.001 Pa and 4.6 ms response time.

The fluidizing gas in all experiments was compressed air regulated to atmospheric pressure using an AW4000 regulator. This enabled precise control of the volumetric flow rate (3.7–2300 mL/min), which was adjusted using one of four Omega float meters connected in parallel. Experiments were performed as follows. First, the particular fluidized bed was filled with one of the four particle grades to one of the three static height ratios. The particles were then emptied from the bed and weighed to confirm the starting weight before being placed back in the bed. Pressure drop data and high-speed videos were then recorded for increasing and decreasing air

flow rates to ensure any hysteresis effects were captured. Here, 20 s of pressure drop data were recorded along with ~3.5 s of high-speed video (corresponding to 2 GB of data) for each air flow rate. Due to the size of the video files, videos were only collected for the 93 ± 10 µm silica and 183 ± 29 µm glass particles, because these were sufficient to show Geldart A and B behaviors respectively.

3. Results to Date

Based on the high-speed video and pressure drop data (average pressure drops and standard deviations), the following flow regimes were identifiable for the gas-solid mini-fluidized beds containing Geldart A and B particles when increasing the gas velocity. Examples of these flow regimes are shown in Figure 2, whilst Figure 3 shows example pressure drop characteristics. Similar observations are reported by Wang *et al* (2011) [5].

- *Packed bed*. Fixed particle bed structure and an almost linear increase of the bed pressure drop with increasing gas velocity. The pressure drop was also very stable, indicating no movement of the particles and no gas bubble formation
- *Minimum fluidization*. Slight bed expansion was observed along with a slight decrease in pressure drop (due to wall effects). The pressure drop remained constant for further increases in gas velocity following the onset of fluidization
- *Bubbling I*. Resembling particulate fluidization, the formation of small gas bubble columns is observed mainly at the wall. Additionally, small gas bubbles are observed across the whole distributor, but these quickly collapse leading to poor mixing
- *Bubbling II*. Consistent bubble formation is observed across the whole distributor. Bubbles rise up to the surface across the full cross-section of the bed and the mixing is qualitatively good. There is also minimal variation in the particle bed height
- *Slugging*. Large gas slugs develop across the majority of the cross-section of the bed due to bubble coalescence. Large variation in the particle bed height occurs as a result of continuous geyser eruptions occurring at the free surface
- *Turbulence*. Bubble and slug formations are no longer visible. The majority of the cross-section of the bed is a homogeneous blend of particles within the gas (there is no clear distinction between bubble and emulsion phases). The particle bed density decreases from the distributor towards the free surface; the bed height remains relatively constant (compared to slugging)
- *Elutriation*. Particles would begin to statically adhere to the walls or reach the terminal velocity resulting in a decrease of the pressure drop. It was not possible to observe any meaningful difference between turbulence and elutriation using high-speed camera data

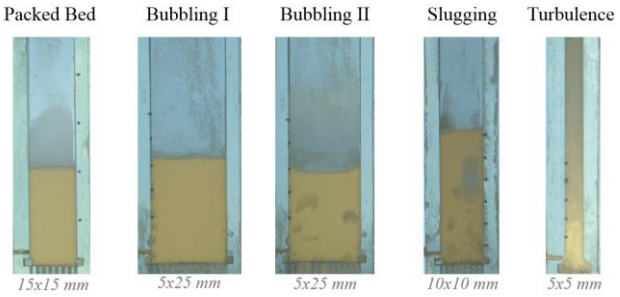

Figure 2. *Images of the identified flow regimes taken from various high-speed videos and fluidized bed configurations*

In Figure 3, it can be seen that the pressure drop initial increases when increasing the gas flow rate. Then, at the minimum fluidization point, the wall friction is overcome resulting in a decrease in the pressure drop. During bubbling, the standard deviation of the pressure drop begins to increase but the pressure drop itself stays constant. Once slugging develops, much larger standard deviations in the signal are observed. Finally, with the onset of turbulence, the standard deviation of the pressure drop decreases.

Using the high-speed video data, the velocities corresponding to flow regime transitions were determined and plotted against the dimensionless size ratio D_h/D_p (hydraulic diameter divided by the particle diameter). The flow regime boundaries shown in Figure 4 were subsequently obtained by connecting each of the resulting points and extrapolating.

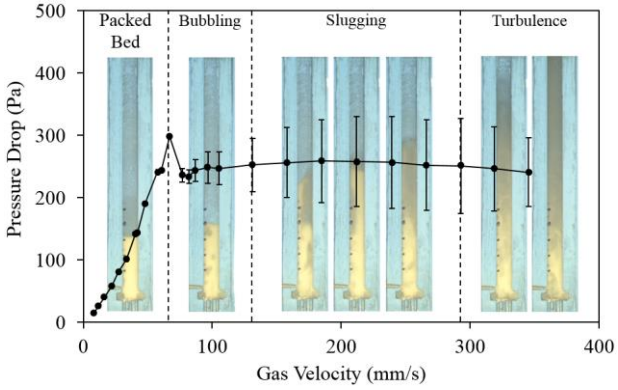

Figure 3. *Example pressure drop behavior | 93 ± 10 µm silica particles in a 5x5 mm fluidized bed | increasing gas flow rate*

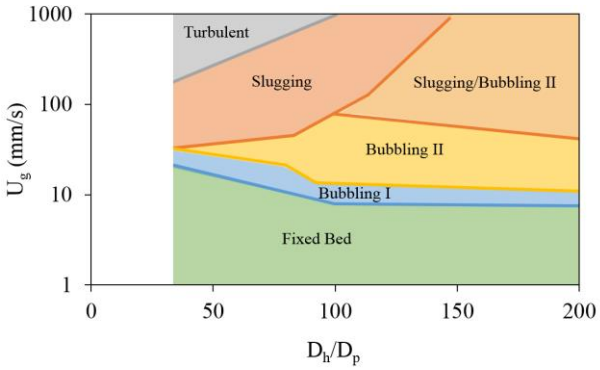

Figure 4. *Preliminary flow regime map derived from high-speed video data of 93 ± 10 µm silica particles (Geldart A)*

4. Ongoing and Future Work

Current work is focused on completion of the data analysis for the refinement of the flow regime boundaries reported in Figure 3. The aim is to produce flow maps for Geldart A and Geldart B particles and observe how the boundaries are influenced by the particle bed height/hydraulic diameter ratio (H_s/D_h). New fluidized bed designs have also been fabricated in order to validate the predicted performance of the flow maps.

Following the completion of the flow regime mapping study, screening of novel tailored hydrotalcites synthesized by a project collaborator (Heriot-Watt University) will be performed using different 3D printed fluidized bed. The goal of these small scale screening experiments is to test the adsorption capability of the solid adsorbents at conditions relevant to industry, and to quantify the effect of flow regime on the adsorption kinetics.

References

[1] Proceedings of the Committee on Climate Change. https://www.theccc.org.uk/tackling-climate-change/the-legal-landscape/european-union-legislation/ (Accessed 4 April 2017)

[2] Reay, D.A. *et al* (2013). Intensification of separation processes. Chapter 6 in: Process Intensification, 2nd Edition, Butterworth-Heinemann, Oxford, pp.205-249.

[3] Berger AH, Horowitz JA, Machalek T, Wang A, Bhown AS (2017) A novel rapid temperature swing adsorption post-combustion CO_2 capture process using a sorbent polymer composite. Energy Procedia 114. 2193-2202

[4] Jaiboon O, Chalermsinsuwan B, Mekasut L, Piumsomboon P (2013) Effect of flow patterns/regimes on CO_2 capture using K_2CO_3 solid sorbent in fluidized bed/circulating fluidized bed. Chemical Engineering Journal 219, 262-272

[5] Wang F and Fan L-S (2011) Gas-solid fluidization in mini- and micro-channels. Industrial & Engineering Chemistry Research 50, 4741-4751